Electrochemical and PM-IRRAS Studies of the Effect of Cholesterol on the Structure of a DMPC Bilayer Supported at an Au (111) Electrode Surface, Part 1: Properties of the Acyl Chains

Xiaomin Bin, Sarah L. Horswell, and Jacek Lipkowski
Department of Chemistry, University of Guelph, Guelph, Ontario, Canada N1G 2W1

ABSTRACT Charge density measurements and polarization modulation infrared reflection absorption spectroscopy were employed to investigate the spreading of small unilamellar vesicles of a dimyristoylphosphatidylcholine (DMPC)/cholesterol (7:3 molar ratio) mixture onto an Au (111) electrode surface. The electrochemical experiments demonstrated that vesicles fuse and spread onto the Au (111) electrode surface, forming a bilayer, at rational potentials $-0.4\ \text{V} < (E - E_{\text{pzc}}) < 0.4\ \text{V}$ or field strength $<6 \times 10^7\ \text{V m}^{-1}$. Polarization modulation infrared reflection absorption spectroscopy experiments provided information concerning the conformation and orientation of the acyl chains of DMPC molecules. Deuterated DMPC was used to subtract the contribution of C-H stretching bands of cholesterol and of the polar head region of DMPC from spectra in the C-H stretching region. The absorption spectra of the C-H stretch bands in the acyl chains were determined in this way. The properties of the DMPC/cholesterol bilayer have been compared with the properties of a pure DMPC bilayer. The presence of 30% cholesterol gives a thicker and more fluid bilayer characterized by a lower capacity and lower tilt angle of the acyl chains.

INTRODUCTION

Biological membranes consist of bilayers formed from phospholipids as the basic building units, and various additional components. One of the most important components of the membrane is cholesterol, which affects the membrane properties significantly (1). For example, it reduces membrane permeability (2–4), alters lateral diffusion rates for both proteins and lipids (5,6), broadens gel-to-liquid crystal lipid phase transitions, and modulates acyl chain order in both gel and liquid crystalline states (7–9). All these changes are related to the interaction between phospholipids and cholesterol, which has attracted a lot of interest. Consequently, a wide variety of physical techniques has been employed to investigate mixed phospholipid and cholesterol monolayer or bilayer mixture systems (1,10,11).

The study of membrane phase behavior, as a function of temperature and concentration of cholesterol, is a focus of numerous studies (10,12–19). In general, pure phospholipid bilayers can exist in four phases and experience three corresponding phase transitions. The subtransition arises from the conversion of the crystalline gel ($L_{c'}$) to the lamellar gel ($L_{\beta'}$) phase, the pretransition from the conversion of the $L_{\beta'}$ phase to the rippled gel ($P_{\beta'}$) phase, and the main transition from a conversion of the $P_{\beta'}$ phase to the lamellar liquid-crystalline (L_α) phase. The existence of cholesterol in the phospholipid bilayer was found to significantly influence its phase behavior. The pretransition and the subtransition disappear as the concentration of cholesterol is increased, the main phase transition region becomes broad, and the main phase transition temperature decreases correspondingly. Simultaneously, a cholesterol-rich gel-like phase ($L_{o\beta}$) appears at temperatures below the main phase transition temperature whereas a cholesterol-rich liquid crystalline phase ($L_{o\alpha}$) appears at temperatures above the main phase transition temperature at high concentrations of cholesterol (20–23).

Despite quite a broad interest in the properties of the phospholipid and cholesterol mixed bilayers, most of these investigations have been performed as a function of temperature or concentration of cholesterol. Natural biological membranes are frequently exposed to static electric fields of the order of 10^7–$10^8\ \text{V m}^{-1}$ (24). However, little is known about how the electric field affects the properties of these membranes. We have recently demonstrated that a phospholipid bilayer deposited on a gold electrode surface can be exposed to static electric fields comparable with that acting on a natural biological membrane (25–29). Bilayers formed by pure phospholipids were interrogated in these studies.

The object of this work was to investigate the effect of cholesterol on properties of a membrane exposed to high electric fields. The model membrane system studied in this work was a mixed dimyristoylphosphatidycholine (DMPC) and cholesterol (70:30 mol% ratio) bilayer formed on an Au (111) electrode surface by fusion and spreading of vesicles. For consistency with previous studies, all experiments were performed at room temperature (20 ± 2°C) at which the DMPC/cholesterol (70:30 mol% ratio) bilayer existed in a gel-like cholesterol-rich phase ($L_{o\beta}$) (22). The formation of the bilayer at the interface was investigated with electrochemical methods. In situ photon polarization modulation infrared reflection absorption spectroscopy (PM-IRRAS) was used to monitor potential-induced reorientation and conformational changes of phospholipid molecules in the

Submitted December 19, 2004, and accepted for publication April 15, 2005.
Address reprint requests to Jacek Lipkowski, E-mail: lipkowski@chembio.uoguelph.ca.

0006-3495/05/07/592/13 $2.00
doi: 10.1529/biophysj.104.058347

bilayer. To assess the effect of cholesterol on the membrane properties, the results for the DMPC/cholesterol mixed bilayer were compared with the results for a pure DMPC bilayer described in a previous article (29). Due to the huge volume of experimental data, this work is divided into two parts. In this article, we analyze the properties of the acyl chains. The behavior of the polar head region of DMPC molecules will be described in the next publication.

EXPERIMENTAL PROCEDURES

Preparation of DMPC/cholesterol vesicles

Vesicles were prepared by the method described by Barenholz et al. (30). Solutions of dimyristoylphosphatidylcholine (deuterated DMPC (d-DMPC), Avanti Polar Lipids, Birmingham, AL; nondeuterated DMPC (h-DMPC), Sigma-Aldrich, St. Louis, MO) and cholesterol (99+%, Sigma-Aldrich) in chloroform (99.9+%, Sigma-Aldrich) were combined in a test tube to form a 7:3 (DMPC/cholesterol) mol fraction mixture. The solvent was evaporated to dryness by vortexing the mixture under a stream of argon. Complete removal of the chloroform was achieved by placing the test tube in a vacuum desiccator for a minimum of 2 h. A sufficient volume of 0.1 M NaF (Merck, Suprapur, Darmstadt, Germany) electrolyte was added to the dry lipid to give an ~1-mg ml^{-1} solution. The mixture was sonicated at 40°C for ~2 h to form vesicles. The solution of vesicles was added to a glass cell using a 1-ml syringe. The final concentration of DMPC was $\sim 1 \times 10^{-4}$ M.

Electrochemical measurements

All electrochemical measurements were carried out in an all-glass three-electrode cell using the working electrode (WE) in a hanging meniscus configuration (31). An Au single crystal with a (111) surface was used as a WE. The counter electrode (CE) was an Au coil and the reference electrode was a saturated calomel electrode (SCE). However, for consistency with spectroscopic measurements and earlier articles from this laboratory, all potentials will be reported versus the Ag/AgCl (3 M KCl) electrode ($E = -40$ mV versus the SCE).

The supporting electrolyte was 0.1 M NaF. This is a nonadsorbing electrolyte that suppresses solubility of the BaF_2 window used in PM-IRRAS experiments. The electrolyte was deaerated by purging argon (BOC Gases, Mississauga, Canada) through the solution for at least 30 min before the measurements. Cyclic voltammetry and differential capacitance measurements of the pure electrolyte were used to check the cleanliness of the system (32). The equipment to perform electrochemical measurements consisted of a Heka potentiostat/galvanostat 600 (HEKA, Lambrecht/Pfalz, Germany) and a 7265 DSP lock-in amplifier (EG&G Instruments, Cypress, CA). All data were acquired via a plug-in acquisition board (RC Electronics, Santa Barbara, CA) and in-house software.

Chronocoulometry was applied to determine the charge density at the electrode surface. The gold electrode was held at a base potential $E_{base} = -0.05$ V for 180 s to allow for complete spreading of vesicles on the electrode surface. The potential was then stepped to a variable potential E_c for a time 180 s, which was long enough to establish a new equilibrium state of the film at the electrode surface. The potential was then stepped to the desorption potential $E_{des} = -1.2$ V (Ag/AgCl) for 0.15 s. Integration of the current transients gives the difference between charge densities at potentials E_c and E_{des}. To measure the charge density for pure electrolyte as a background, the same set of experiments was performed at the Au (111) electrode in the solution without DMPC/cholesterol vesicles. The absolute charge densities were calculated using a potential of zero charge (pzc) $E_{pzc} = 0.30$ V versus Ag/AgCl. The solutions were stirred to enhance mass transport to the electrode. Stirring was interrupted ~10 s before stepping the potential to E_{des}. Surface pressures were calculated by integration of the charge density curves.

Spectral collection and processing

The PM-IRRAS setup consisted of a Nicolet Nexus 870 spectrometer, equipped with an external optical bench, MCT-A detector TRS50 MHz (Nicolet, Madison, WI), photoelastic modulator (PEM) (Hinds Instruments PM-90 with II/ZS50 ZnSe 50 kHz optical head, Hillsoboro, OR), and a demodulator (GWC Instruments synchronous sampling demodulator, Madison, WI). The electrode potentials were controlled via a potentiostat (EG&G, PAR model 362) using in-house software, an Omnic Macro and a digital-to-analog converter (Omega, Stamford, CT). In addition, an Omnic Macro was used to collect and save spectra. The infrared (IR) window was a BaF_2 1-inch equilateral prism. The window was washed with methanol and water and then cleaned in an ozone ultraviolet chamber (UVO-cleaner, Jelight, Irvine, CA) for 20 min before cell assembly. Details concerning the PM-IRRAS spectroelectrochemical cell have been described elsewhere (33). DMPC/cholesterol vesicles prepared in either D_2O or H_2O were injected into the electrolyte-filled cell and the solution was deaerated with argon for 2 h before measurement. The vesicles were allowed to fuse and spread to form a bilayer on the surface of the working electrode. The potential of the WE was set initially at −1.0 V versus Ag/AgCl and spectra were then acquired at a series of potentials, which were programmed as a cyclic sequence of 0.1 or 0.2 V potential steps. In total, 20 cycles of 400 scans each were performed to give 8000 scans at each applied potential. The resolution of the instrument was 2 cm^{-1}. At the end of the experiment, blocks of scans were individually checked for anomalies before averaging using in-house software.

Measurements of IR spectra were carried out with the PEM set at half-wave retardation at 2900 cm^{-1} for the C-H stretching region and 2100 cm^{-1} for the C-D stretching region, respectively. To avoid the large absorption from the electrolyte background, D_2O was used as the solvent for the measurements in the 2900 cm^{-1} spectral region and H_2O was used for the 2100 cm^{-1} region. The incident angle of the IR beam was set at 53° and the thickness of the electrolyte between the prism and electrode was 5.8 μm for the C-H stretching region. These parameters gave comparable intensities of p- and s-polarized light inside the thin layer cavity and hence allow for the cancellation of the IR absorption by vesicles that remained in the solution without spreading on the electrode surface. For the C-D stretching region, the incident angle was 60° and the gap thickness was also 5.8 μm.

The demodulation technique developed in Corn's laboratory was applied in this work (34). A modified version of a method described by Buffeteau et al. (35) was used to correct the average intensity $I_A(\omega)$ and the intensity difference $I_D(\omega)$ for the PEM response functions and for the difference in the optical throughputs for p- and s-polarized light. Finally, the measured spectra had to be background corrected due to the absorption of IR photons in the thin layer cavity. The spline interpolation technique described by Zamlynny et al. (36) was used for this background correction. After all these corrections, the background-corrected spectrum is a plot of $\Delta S(\omega)$, which is the absorbance of the film of adsorbed molecules:

$$\Delta S(\omega) = \frac{(I_s - I_p)}{(I_s + I_p)/2} = 2.3\ A = 2.3\ \Gamma\varepsilon, \qquad (1)$$

where ε is the decimal molar absorption coefficient and Γ is the surface concentration of the absorbing molecules.

To determine the angle between the direction of the transition dipole of a given vibration and the surface normal, the absorbance of a hypothetical bilayer consisting of randomly oriented molecules $A_{(random)}$ had to be calculated. For that purpose, the optical constants for the acyl chains in the mixed h-DMPC/h-cholesterol bilayer were determined from transmission spectra using the procedure described (36–38). The transmission spectra of h-DMPC/h-cholesterol and DMPC-d_{54}/h-cholesterol vesicles in D_2O and H_2O and solutions of these mixtures in CCl_4 were measured in a flow cell, consisting of two BaF_2 flat windows separated by a 25-μm-thick Teflon spacer. The attenuation coefficient k for the acyl chains was determined by calculating k for the h-DMPC/h-cholesterol and DMPC-d_{54}/h-cholesterol mixtures from transmission spectra and taking the difference between the two k values. The refractive index n was calculated from k for the chains

using the Kramers-Kroenig transformation. The average refractive index at infinite frequency $n_\infty = 1.4$ was used for the whole spectral region (39,40).

The $A_{(\text{random})}$ values were then calculated from the optical constants using the optical matrix method for reflection from an interface consisting of four phases: Au/DMPC/D_2O or H_2O/BaF_2 (36,38). The optical constants for Au and BaF_2 were taken from Palik (41), whereas the optical constants for D_2O and H_2O were taken from Bertie et al. (42). The angle of incidence was 53° and the thickness of the thin layer cavity was 5.8 μm. They were determined using the procedure described in Li et al. (38). The thickness of the film of randomly oriented molecules was assumed to be equal to 5.5 nm, which is the thickness of the mixed DMPC/cholesterol bilayer measured by the neutron diffraction method (43). The spectra calculated from the optical constants determined from transmission measurements for vesicles in D_2O and a DMPC-cholesterol solution in CCl_4 are plotted with thick lines in figures presenting PM-IRRAS spectra for the bilayer formed by fusion of vesicles.

Error analysis

To estimate the error in the determination of the tilt angle of the acyl chains, one has to consider the possible errors that arise in each step of the entire spectral data analysis procedure. Three factors can contribute to the net error of the calculated tilt angles: 1), the errors in the absorbance A_{exp} in reflection absorption spectroscopy and the error in absorbance A_{cal} calculated using the experimentally determined optical constants; 2), the error from the background correction procedures; 3), the error from the deconvolution procedure. An estimate of all these errors gives the final uncertainty of the tilt angle ±2°. This estimate is consistent with the observed spread of the experimental points.

RESULTS AND DISCUSSION

Electrochemical properties

The behavior of the mixed DMPC/cholesterol bilayer on an Au (111) electrode surface was characterized first with charge density-potential plots. For comparison, the data for the mixed bilayer and pure DMPC bilayer are presented jointly. The measurements for the DMPC/cholesterol mixture and pure DMPC were performed under similar conditions. They refer to spreading of phospholipids at a nonreconstructed Au (111) surface. The electrochemical data for DMPC presented here are different from those shown by Bin et al. (29) for a reconstructed Au (111) surface. The differences reflect the effect of the surface crystallography and a different choice of the base potential: −0.05 V in this study and −0.8 V in the article by Bin et al. (29). At $E = -0.8$ V the bilayer interacts very weakly with the gold surface and hence a fraction of the bilayer can easily drift away and be lost in the bulk of the electrolyte. To prevent such losses, in this work the base potential was changed to −0.05 V where the bilayer is firmly attached to gold.

Fig. 1 *a* plots the charge density curves for pure DMPC and DMPC/cholesterol mixtures. In the potential region of $-0.4 < E < 0.4$ V, the absolute value of charge density at the Au (111) electrode surface is much smaller in the presence of vesicles than in the vesicle-free solution. This behavior indicates that vesicles fuse and form a film at the gold surface. The absolute value of the charge at the electrode

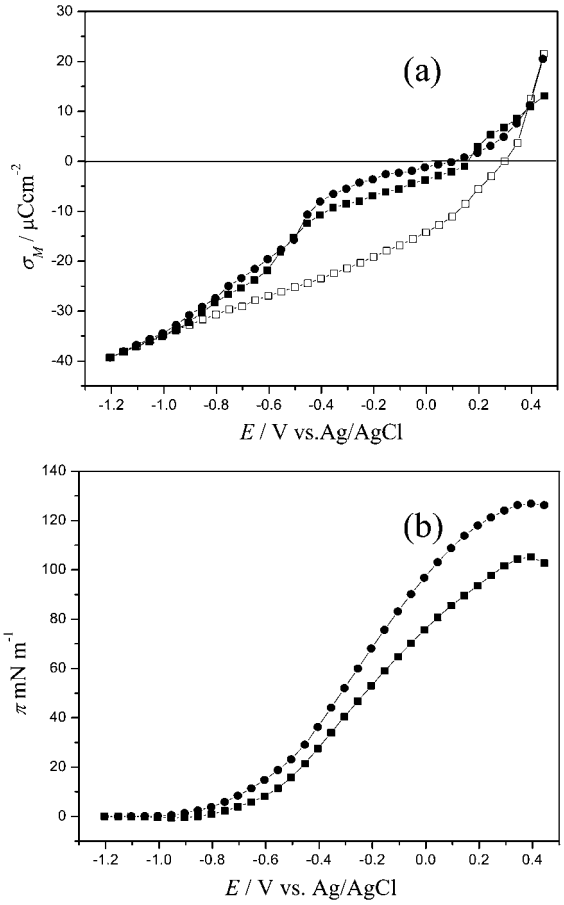

FIGURE 1 (*a*) Surface charge density on the gold electrode plotted versus electrode potential for (□) 0.1 M NaF supporting electrolyte, (■) pure DMPC bilayer, and (●)mixed 7:3 DMPC/cholesterol bilayer spread from a vesicle solution. (*b*) Surface pressure π versus potential plot calculated by integration of the charge density curves: (■) pure DMPC bilayer and (●) mixed 7:3 DMPC/cholesterol bilayer spread from the vesicle solution.

covered by the DMPC/cholesterol film is smaller than that of the electrode covered by the film of pure DMPC, indicating that a film with lower capacity is formed when cholesterol is mixed with DMPC.

At $E > 0.5$ V, hydroxide adsorption and gold oxide formation begin. The experiments were therefore restricted to $E < 0.5$ V. At $E < -0.4$ V, the difference between the charge densities measured for the Au (111) electrode in solution with and without vesicles decreases and at the most negative potentials the charge density curves merge, indicating that the film is detached (desorbed) from the gold surface. Independent neutron reflectivity experiments have shown that when the bilayer is detached from the electrode surface at negative potentials, it remains in close proximity to the electrode, separated from the gold surface by an ~1-nm-thick layer of electrolyte (28).

The area between the charge density curves for the supporting electrolyte and the electrolyte containing DMPC or DMPC/cholesterol mixed vesicles corresponds to the

surface pressure of the bilayer, which can be calculated using the following equation (44,45):

$$\pi = \gamma_0 - \gamma = \int_{E=-1.25V}^{E} \sigma_M dE - \int_{E=-1.25V}^{E} \sigma_{M_0} dE, \quad (2)$$

where γ_0 and γ are the surface energies (γ is the work done to create a unit area of a solid surface by cleavage) and σ_{M_0} and σ_M are the charge densities in the absence and presence of vesicles in the solution, respectively.

The surface pressure curves are shown in Fig. 1 *b*. The surface pressure quantitatively describes the energetics of spreading the vesicles to form a membrane at the metal-solution interface. The surface pressure plot is bell-shaped with a maximum of 125 mN m^{-1} at $E = 0.35$ V for the DMPC/cholesterol mixture and 105 mN m^{-1} at $E = 0.45$ V for the pure DMPC. The equilibrium film pressure of a monolayer of the DMPC/cholesterol mixture and pure DMPC at the interface between air and the solution of vesicles amounts to 52 and 47 mN m^{-1}, respectively. Therefore, the maximum pressure of the film at the electrode surface is close to the double of the pressure of a monolayer. This number is consistent with the formation of a bilayer. In fact, recent neutron reflectivity experiments demonstrated that a bilayer is formed when mixed DMPC/cholesterol vesicles are fused at a gold electrode surface (28).

The film pressure for the DMPC/cholesterol bilayer is higher than for the bilayer of pure DMPC. This result shows that the addition of cholesterol results in the formation of a more compact membrane. Independent AFM experiments performed on the same systems indicate that the bilayer formed from pure DMPC vesicles exhibits a ripple phase, which contains many defects and may be seen as an assembly of rafts separated by cracks filled with the solvent. In contrast, AFM images for the DMPC/cholesterol mixed bilayer showed a smooth film (46). This observation is consistent with differential scanning calorimetric data that have shown that the ripple phase of phospholipid bilayers disappears with the incorporation of >5% (mol%) cholesterol (20,47).

The charge density curves can be used to estimate the potential drop between the metal and the bulk electrolyte solution ($\Delta\phi_{M-S}$), which is approximately equal to the potential drop across the membrane, using the formula (48):

$$\Delta\phi_{M-S} = \frac{\sigma_M}{C} + \chi_M, \quad (3)$$

where χ_M is the surface potential of the membrane. The capacity C can easily be calculated by differentiation of the charge density curve.

Fig. 2 plots σ_M/C calculated from the charge density curves, for potentials where the bilayers are directly adsorbed at the gold surface. These potentials are equivalent to the transmembrane potentials applied to a membrane in the patch clamp or bilayer lipid membrane experiment. The open points in Fig. 2 plot the rational potential ($E - E_{pzc}$) where

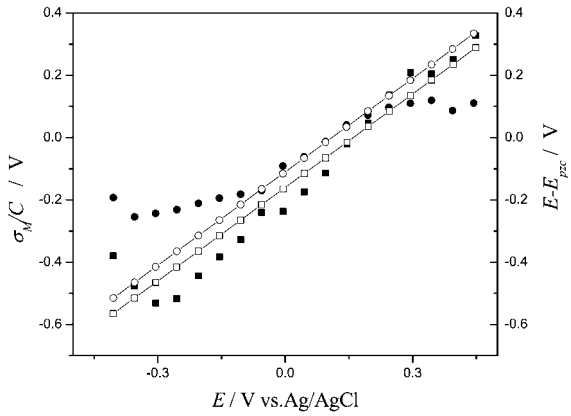

FIGURE 2 The σ_M/C component of the potential drop across the membrane ($\Delta\phi_{M-S}$) and ($E - E_{pzc}$) as a function of applied potential E. (■)σ_M/C component for the pure DMPC bilayer and (●) for the mixed 7:3 DMPC/cholesterol bilayer spread from the vesicle solution. (-□-) ($E - E_{pzc}$) for the pure DMPC bilayer and (-○-) for the mixed 7:3 DMPC/cholesterol bilayer spread from the vesicle solution.

E_{pzc} is the potential of zero charge in a given solution of vesicles (E_{pzc} is equal to 0.156 V in the presence of DMPC and 0.110 V in the presence of a DMPC/cholesterol mixture). As expected, the values of σ_M/C are comparable with the values of the rational potential. The results show that the bilayers are adsorbed at the gold surface when the absolute value of σ_M/C is <0.4 V. However, the neutron reflectivity experiments indicate that the adsorbed bilayer swells and absorbs water at $E < -0.3$ V versus Ag/Ag/Cl. This suggests that the compact bilayer exists when the transmembrane potential is <0.3 V, in good agreement with the magnitude of the transmembrane potential applied to bilayer lipid membranes in membrane conductivity measurements (49). Considering that the thickness of a membrane bilayer is ~5 nm, the electric field across the bilayer changes between $\sim -6 \times 10^7$ V m^{-1} and $\sim +6 \times 10^7$ V m^{-1} in this potential region. The amplitude of this electric field is comparable with the field acting on a natural membrane (24).

The adsorption of phospholipid molecules onto the Au electrode surface causes a small shift of the pzc in the negative direction, ~180 mV for the DMPC/cholesterol mixture and ~134 mV for pure DMPC, as shown in Fig. 1 *a*. The shift of the pzc (E_N) is described by $E_N = \Gamma(\mu_\perp^{org} - n\mu_\perp^w)/\varepsilon$ (45), where Γ is the surface concentration of organic molecules, ε is the permittivity, $\mu_\perp^{org}$ and $\mu_\perp^w$ are the components of the permanent dipoles of the organic and water molecules in the direction normal to the surface, and n is the number of water molecules displaced from the surface by one organic molecule. At the pzc of the Au (111)/solution interface, water molecules are expected to have a small preferential orientation with the oxygen atom directed toward the metal and hence $\mu_\perp^w$ should be rather small (50) and its sign should be negative. Therefore, the absolute value of the dipole potential due to the orientation of permanent dipoles of phospholipid molecules ($\mu_\perp^{org}$) should be

somewhat higher than 150 mV. In this case $\mu_{\perp}^{org}$ is likely to be related to the asymmetric environment of the two leaflets of the bilayer, one facing the metal and the other the bulk of the solution. This estimate agrees reasonably well with the value of the surface potential in free-standing bilayers of phosphatidylcholines, estimated to be ~280 mV (51–53).

Fourier transform infrared studies

In the following section the infrared spectra of DMPC bilayers containing 30% cholesterol under the influence of a static electric field are discussed and compared with those of pure DMPC bilayers described by Bin et al. (29). A DMPC molecule contains 24 methylene groups and two terminal methyl groups in two acyl chains, and four methylene groups in the head moiety. A cholesterol molecule contains three methylene groups in the alkyl chain, seven methylene and seven CH groups in the four cyclic rings and five methyl groups. For a DMPC/cholesterol (7:3 molar ratio) system, the DMPC bands are dominant, as the cholesterol bands are about an order of magnitude weaker. The bulk of the data were collected for the bilayer of nondeuterated molecules (h-DMPC/h-cholesterol mixture). However, additional measurements were performed for a mixture of DMPC with deuterated acyl chains and nondeuterated CH_2 groups in the head moiety with nondeuterated cholesterol (DMPC-d_{54}/h-cholesterol). The difference between the spectra obtained for the h-DMPC/h-cholesterol and DMPC-d_{54}/h-cholesterol mixed bilayers then provided information exclusively related to the C-H vibrations in the two acyl chains of the h-DMPC molecule. In addition, the C-D vibration bands provided complementary information concerning the deuterated hydrocarbon chains in the DMPC-d_{54}/h-cholesterol system.

Vibrations of nondeuterated chains in the h-DMPC/h-cholesterol mixture

Experiments described in this section were carried out with D_2O as the solvent. Fig. 3 *a* shows the IR spectra in the CH stretching region for the pure DMPC and DMPC/cholesterol mixtures. In each case, the top two thicker lines represent the bilayer of randomly oriented molecules, calculated from the transmission spectra of a solution of phospholipids in CCl_4 and a dispersion of phospholipid vesicles in D_2O, respectively. The four thinner curves below plot the PM-IRRAS spectra for the bilayer of phospholipids at the electrode surface at selected electrode potentials. There are four normal mode bands corresponding to the asymmetric $\nu_{as}(CH_3)$, $\nu_{as}(CH_2)$ and symmetric $\nu_s(CH_3)$ and $\nu_s(CH_2)$ stretches, and two Fermi resonances between the overtones of the symmetric bending mode and symmetric methyl and methylene stretches (54) in this spectral region.

The addition of 30% cholesterol affects the position, width, and intensity of the CH_2 stretch bands significantly. These changes may result from a change of the total number of the CH_2 groups, a change in the number of *gauche* conformations, or a change of the tilt angle of the acyl chains in the DMPC molecules. To separate these effects we have performed an additional experiment using DMPC molecules with perdeuterated acyl chains (DMPC-d_{54}). This molecule has fully deuterated acyl chains but the four methylene groups in the polar head region and the methyl groups of the choline moiety contain hydrogen atoms. Fig. 3 *b* plots spectra in the C-H stretch region for the DMPC-d_{54}/h-cholesterol mixed system. Again, the top two thick lines plot the spectra for the CCl_4 solution and the aqueous dispersion of vesicles. The bottom curves plot the spectra for the bilayer adsorbed on the Au (111) electrode surface at selected electrode potentials. The band intensities in this spectral

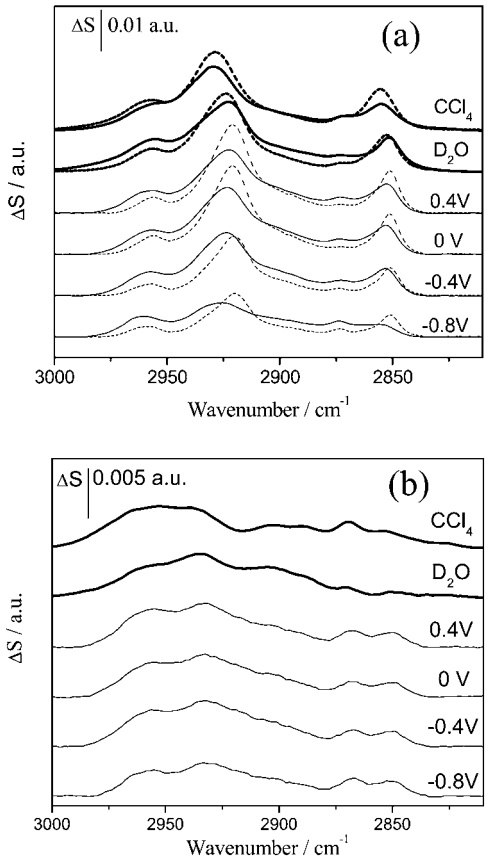

FIGURE 3 (*a*) PM-IRRAS spectra in the CH stretching region of the h-DMPC bilayer (*dashed line*) and the mixed 7:3 h-DMPC/cholesterol bilayer (*solid line*) on an Au (111) electrode surface in 0.1 M NaF/D_2O solution at potentials indicated on the figure. The top two traces plot spectra calculated for a 5.5-nm-thick film of randomly oriented molecules, using the optical constants for h-DMPC or h-DMPC/cholesterol (7:3) mixtures for solutions in CCl_4 (*top line*) and vesicle dispersions in D_2O (*second line*). (*b*) PM-IRRAS spectra in the CH stretching region of the mixed 7:3 DMPC-d_{54}/h-cholesterol on an Au (111) electrode surface in 0.1 M NaF/D_2O solution at potentials indicated on the figure. The top two traces plot spectra calculated for a 5.5-nm-thick film of randomly oriented molecules, using the optical constants for the DMPC-d_{54}/h-cholesterol (7:3) mixture determined from transmission spectra of a solution in CCl_4 (*top line*) and a vesicle dispersion in D_2O (*second line*). Abbreviation a.u. denotes absorbance units.

region are obviously much weaker than for the h-DMPC/h-cholesterol mixture presented in Fig. 3 *a*.

The difference between the spectra measured for the bilayer of nondeuterated molecules (h-DMPC/h-cholesterol) and the bilayer of DMPC with perdeuterated tails (DMPC-d_{54}/h-cholesterol) gives the spectra for C-H stretch modes of the acyl chains only, assuming that the physical state (phase) of the acyl chains does not affect the conformation of the headgroups or cholesterol molecules. The spectra of the acyl chains are plotted in Fig. 4 *a*. The deconvolution of this spectral region into $\nu_{as}(CH_3)$, $\nu_{as}(CH_2)$ and symmetric $\nu_s(CH_3)$ and $\nu_s(CH_2)$ stretches and two Fermi resonances is shown in Fig. 4 *b*. The CH stretch bands contain valuable information concerning the conformation and orientation of the acyl chains and the physical state of the bilayer. In the following, we shall discuss chiefly the changes of the position, the width, and the intensity of the $\nu_s(CH_2)$ band. When needed, we shall also show some of the data for the $\nu_{as}(CH_2)$ and $\delta(CH_2)$ modes.

The potential dependences of the band position and the full width at half-maximum (FWHM) of the symmetric CH_2 stretching mode ($\nu_s(CH_2)$) in the bilayer of pure DMPC and h-DMPC/cholesterol mixtures are plotted in Fig. 5, *a* and *b*, respectively. The frequency of this band depends on the average number of *gauche* conformers in the system (55). A frequency of the band center of $<2850\ cm^{-1}$ for $\nu_s(CH_2)$ is characteristic of the gel state of the bilayer, in which the acyl chains are fully stretched and assume an all-*trans* conformation. The presence of *gauche* conformers shifts the band to higher frequency and induces higher fluidity of the bilayer. Higher fluidity of the bilayer increases the FWHM of the ($\nu_s(CH_2)$ band (56–59).

For the pure DMPC bilayer, the $\nu_s(CH_2)$ band position is located at 2851.5 cm^{-1} when the bilayer is detached from the Au (111) electrode surface at negative potentials. A slight blue shift to 2852.0 cm^{-1} was observed when the bilayer was adsorbed at the Au (111) electrode surface at positive

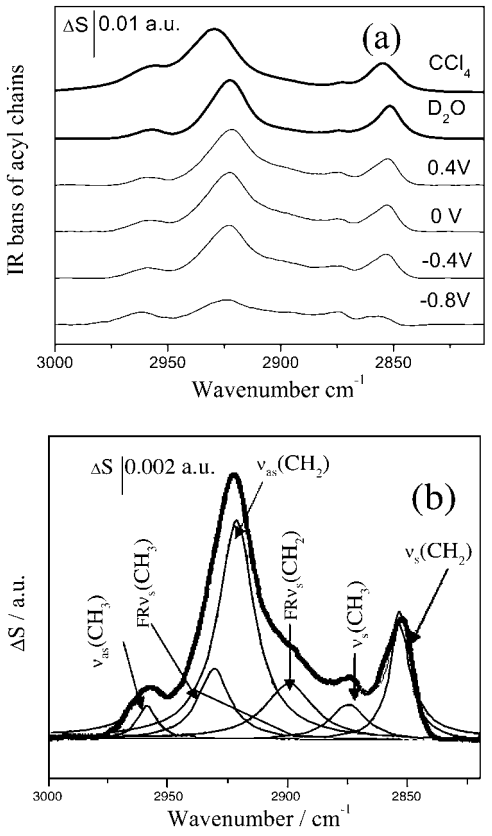

FIGURE 4 (*a*) IR bands of the acyl chains of DMPC/cholesterol mixed bilayers on an Au (111) electrode surface in 0.1 M NaF/D_2O solution at the indicated potentials. The top two thicker traces plot spectra for a 5.5-nm-thick film of randomly oriented molecules, calculated from optical constants determined from transmission spectra of a solution in CCl_4 (*top line*) and a vesicle dispersion in D_2O (*second line*). (*b*) Example of a deconvolution of the overlapping ν_{as} (CH_3), $\nu_{as}(CH_2)$, ν_s (CH_3), ν_s (CH_2) bands and two Fermi resonances between the overtones of the symmetric bending mode and symmetric methyl and methylene stretching modes for the DMPC/cholesterol mixed bilayer at $E = -0.2$ V. Abbreviation a.u. denotes absorbance units.

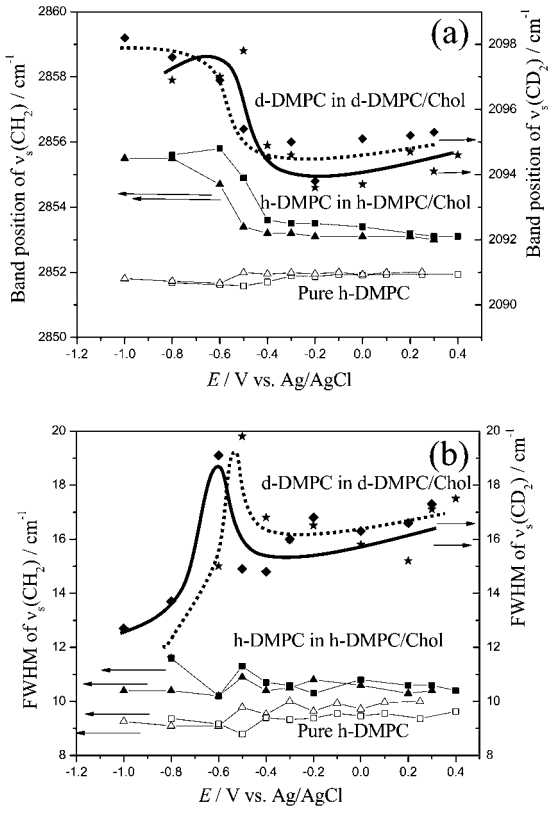

FIGURE 5 (*a*) ν_s (CH_2) band center positions and (*b*) the FWHM as a function of electrode potential. (△, potential changed in negative direction) and (□, potential changed in positive direction) for the pure h-DMPC bilayer; (▲, potential changed in the negative direction) and (■, potential changed in the positive direction) for the mixed 7:3 h-DMPC/cholesterol bilayer. (◆, potential moved in the negative direction) and (★, potential moved in the positive direction) show $\nu_s(CD_2)$ band center (*a*) and FWHM (*b*) for the DMPC-d_{54}/h-cholesterol bilayer.

potentials. The frequencies of the $\nu_s(CH_2)$ band for the pure DMPC bilayer are characteristic of the ripple phase (60) in which the acyl chains of the DMPC molecules are predominantly in the all-*trans* conformation with a small fraction of the chains being melted (60).

The small shift of the band position to higher frequencies (by 0.5 cm^{-1}) at positive potentials is accompanied by a small increase of the FWHM from 9 to 9.5 cm^{-1}. This behavior indicates a small increase in the number of *gauche* conformations and a concomitant increase in fluidity of the film. In the dispersion of vesicles in D_2O, the band frequency was 2853.5 cm^{-1} and its FWHM was 12 cm^{-1}. Therefore, the bands in the bilayer supported at the Au (111) electrode are narrower and red-shifted with respect to the band in vesicles, indicating that, relative to the vesicles, the supported bilayer has fewer *gauche* conformations and is less fluid.

The incorporation of cholesterol into the bilayer results in several effects. In general, the $\nu_s(CH_2)$ bands have higher frequencies and are broader for the h-DMPC/cholesterol mixed bilayer than for the pure DMPC bilayer. This behavior is consistent with the fact that cholesterol increases the average number of *gauche* conformers in the system in the gel phase (8). However, as Fig. 5, *a* and *b*, show, the changes of the band position with the electrode potential are in the opposite direction to the changes observed for the bilayer of pure DMPC. In the desorbed state at negative potentials, the band position is ~2855.5 cm^{-1}. In the adsorbed state at positive potentials, a red shift of the band position to ~2853 cm^{-1} is observed. The FWHM is approximately equal to ~10.5 cm^{-1} and is essentially independent of potential. In the dispersion of vesicles, the $\nu_s(CH_2)$ band frequency is 2852 cm^{-1} and its FWHM is equal to 11 cm^{-1}. Apparently, the $\nu_s(CH_2)$ band positions for the bilayer have higher frequencies although similar widths to the bands for the suspension of vesicles in D_2O.

The frequency shift with potential is more pronounced for the h-DMPC/h-cholesterol mixture than for the pure DMPC bilayer. Recent differential scanning calorimetry data (21) indicate that at a temperature of 20 ± 2°C, a DMPC bilayer containing 30% cholesterol is a mixture of two phases, a liquid-ordered gel-like phase ($L_{o\beta}$) and liquid ordered liquid-crystalline-like phase ($L_{o\alpha}$). These results suggest that the fraction of $L_{o\alpha}$ and $L_{o\beta}$ phases changes with the electrode potential. The fraction of the $L_{o\alpha}$ phase appears to be higher at negative potentials, where the bilayer is separated from the metal by a cushion of solvent, and decreases at positive potentials, when the bilayer becomes directly adsorbed at the metal surface.

The spectra in Fig. 4 show that the intensity of the CH_2 stretch bands of the h-DMPC molecule changes significantly with the electrode potential. Such a change may result either from a change in the number of *gauche* conformations or from the change in the orientation of the acyl chains. To separate these two effects, additional transmission measurements for a suspension of DMPC vesicles as a function of temperature ranging from 20 to 28°C have been performed. The phase transition from the gel to the liquid crystalline state takes place in the middle of this range, at 24°C. The integrated intensities of the $\nu_{as}(CH_2)$ and $\nu_s(CH_2)$ have been calculated and plotted against the band frequency (data not shown). The results have shown that the change in the conformational state changes the integrated band intensity by <2%. This change is negligible and in the following data analysis, we have considered that the potential-driven changes of the band intensity reflect a change in the orientation of the acyl chains.

The orientation of the acyl chains with respect to the surface normal can be determined from the integrated band intensity, which is proportional to the dot product between the transition dipole moment vector (μ) and the electric field vector (E) (36,37,61):

$$\int A dv \propto |\mu \cdot E|^2 = \cos^2\theta |\mu|^2 \langle E^2 \rangle, \tag{4}$$

where θ represents the angle between the direction of the transition dipole and the electric field of the photon (which is normal to the surface). The angle θ can be calculated from the intensity of a hypothetical film consisting of randomly oriented molecules determined from an independent experiment (26,27,29,36,37) as described in the experimental section. Knowing the band intensity for a film of randomly oriented molecules, the tilt angle θ can be then calculated with the formula:

$$\cos^2\theta = \frac{1}{3}\frac{\int A_{(E)} dv}{\int A_{(random)} dv}, \tag{5}$$

where $A_{(E)}$ and $A_{(random)}$ are the absorbances of the IR bands for the bilayer at the electrode surface and for the hypothetical bilayer consisting of randomly oriented molecules.

Fig. 6, *a* and *b*, are plots of the angles between the directions of the transition dipoles of the symmetric and asymmetric methylene stretches and the surface normal, calculated from the integrated band intensities with Eq. 5. The cartoons alongside this figure show the positions of the transition dipoles with respect to the acyl chain of the phospholipid molecule. The transition dipoles of the two stretches are located in the plane of the methylene group. The transition dipole of the $\nu_s(CH_2)$ is oriented along the group diagonal. The transition dipole of the $\nu_{as}(CH_2)$ is perpendicular to the diagonal and is aligned along the direction joining the two hydrogen atoms of this group (62).

The transition dipole of the $\nu_s(CH_2)$ band has the same direction as the transition dipole of the bending band ($\delta(CH_2)$) at 1468 cm^{-1}. The angle for the transition dipole of the $\delta(CH_2)$ is plotted in Fig. 6 *c*. The bending band is weaker than the $\nu_s(CH_2)$, hence the experimental values of θ for this band are subject to larger errors. As expected, similar changes of θ are observed for the symmetric stretch and the

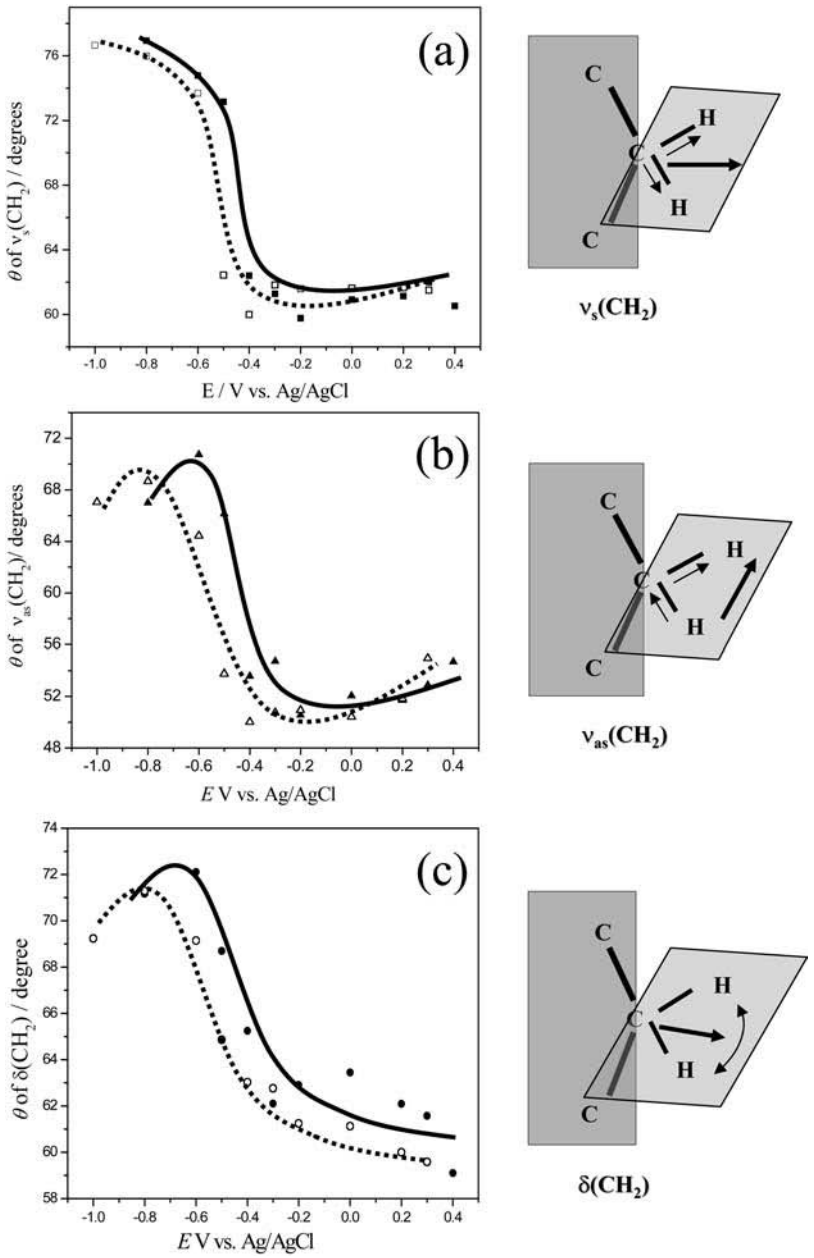

FIGURE 6 (*a*) The potential dependence of the angle (θ) between the directions of the transition dipole moment and the electric field of the photon (normal to the surface) for the mixed DMPC/cholesterol bilayer on the Au (111) electrode in 0.1 M NaF/D_2O solution for: (*a*) $\nu_s(CH_2)$ (■) potential changed in the positive direction, (□) potential changed in the negative direction; (*b*)$\nu_{as}(CH_2)$ (▲) potential changed in the positive direction, (△) potential changed in the negative direction; (*c*) $\delta(CH_2)$ (●) potential changed in the positive direction, (○) potential changed in negative direction.

bending band and their values differ on average by $<4°$. This result indicates that similar structural information can be extracted from IR bands located in different spectral regions. The angle between the directions of the transition dipoles of the CH_2 stretching and bending vibrations and the surface normal decreases abruptly in the potential region of -0.6 V $< E < -0.4$ V, where adsorption of the bilayer at the electrode surface takes place. Apparently, the phospholipid molecules reorient on forming a bilayer directly adsorbed on the Au (111) electrode surface.

When the acyl chains are fully stretched in the all-*trans* conformation, the transition dipole moments of the two methylene stretches are not only perpendicular to each other but are also perpendicular to the line of the hydrocarbon chain, and angles θ_s, θ_{as}, and θ_{chain} are related by the formula (63):

$$\cos^2\theta_{as} + \cos^2\theta_s + \cos^2\theta_{chain} = 1. \quad (6)$$

In this case, a certain number of the acyl chains in the mixed DMPC-bilayer are melted and have *gauche* conformations. Under these conditions, Eq. 6 may only be used to calculate the chain tilt angle as an approximation. Fig. 7 plots the chain tilt angle as a function of the applied potentials. The solid dots and triangles show the tilt angle for the hydrocarbon chains of the DMPC/cholesterol mixed bilayer; the empty dots and triangles show the tilt angle of

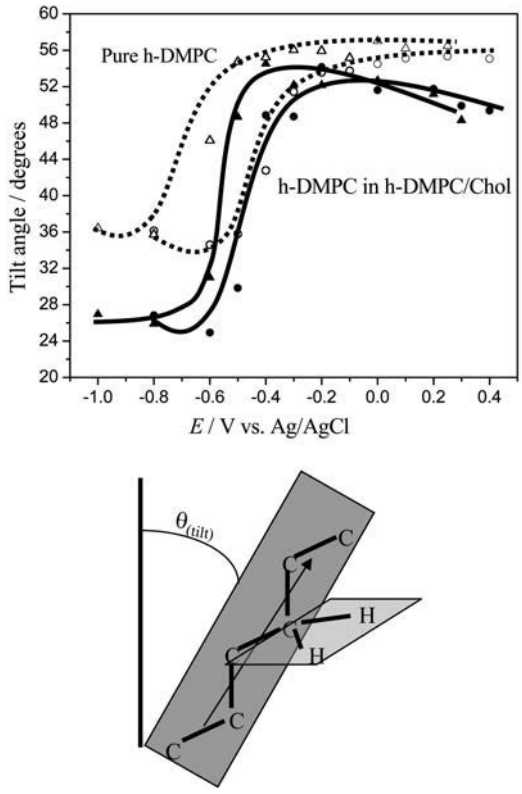

FIGURE 7 Dependence of the tilt angle of the acyl chains on the electrode potential for the pure DMPC bilayer; dashed lines, (○) potential changed in the positive and (△) potential changed in the negative direction. Solid lines, (●) and (▲) denote corresponding changes of the tilt angle for the mixed h-DMPC/h-cholesterol bilayer.

hydrocarbon chains for pure DMPC bilayers on the Au (111) electrode surface, respectively.

The tilt angle changes significantly with the electrode potential. At $E < -0.6$ V, where the bilayer is detached from the metal surface, the tilt angle is ~25° for h-DMPC/cholesterol mixed bilayers and ~35° for pure DMPC bilayers. The tilt angle changes to ~52° for the DMPC/cholesterol mixed film and to ~55° for the pure DMPC at $E > -0.4$ V, where the bilayer is directly adsorbed at the metal surface. The incorporation of 30% cholesterol into the bilayer leads to a decrease of the tilt angle of the acyl chains both in the desorbed and absorbed states. This indicates that the bilayer containing cholesterol is thicker than the bilayer of pure DMPC. This result is in agreement with the previous x-ray diffraction (1,64) or neutron diffraction (43) studies performed on vesicles or multilayers.

Vibrations of deuterated chains in DMPC-d_{54}/h-cholesterol mixture

The experiments described in this section were carried out using H_2O as the solvent. The temperature of the gel-liquid crystalline state phase transition is 18°C for deuterated DMPC (4,65), whereas it is 24°C for nondeuterated DMPC (66). Because our measurements were carried out at 20 ± 2°C, the bilayers of nondeuterated and deuterated DMPC were in different physical states. Nevertheless, it is interesting to extract additional structural information from the analysis of CD stretch bands in the DMPC-d_{54}/h-cholesterol bilayer. Fig. 8 *a* plots the CD stretch bands in the spectral region between 2000 and 2300 cm^{-1}. The top two lines plot the bands for the bilayer of randomly oriented molecules, calculated from the optical constants determined with the help of transmission spectra of a solution of DMPC-d_{54} in CCl_4 and a dispersion of DMPC-d_{54} vesicles in H_2O, respectively. The four bottom curves plot the PM-IRRAS spectra for the bilayer of DMPC-d_{54}/h-cholesterol at the electrode surface at selected electrode potentials. This spectral region consists of four overlapping bands corresponding to $\nu_{as}(CD_3)$, $\nu_{as}(CD_2)$, $\nu_s(CD_3)$, and $\nu_s(CD_2)$ and two Fermi resonances between $\nu_s(CD_3)$ and

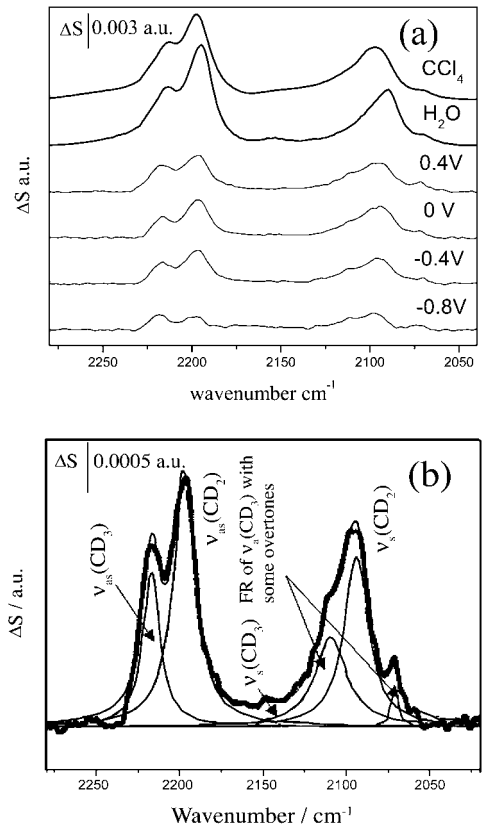

FIGURE 8 (*a*) PM-IRRAS spectra for the CD stretching region of a mixed DMPC-d_{54}/h-cholesterol bilayer on an Au (111) electrode in 0.1 M NaF/H_2O solution at the indicated potentials. The top two traces plot spectra calculated for a 5.5-nm-thick film of randomly oriented molecules, using optical constants for DMPC-d_{54}/h-cholesterol (7:3) determined from transmission spectra of the solution in CCl_4 (*top line*) and the dispersion of vesicles in H_2O (*second line*). (*b*) Example of a deconvolution of the overlapping ν_{as} (CD_3), $\nu_{as}(CD_2)$, ν_s (CD_3), ν_s (CD_2) bands and two Fermi resonances between overtones and symmetric methyl ($\nu_s(CD_3)$) modes for the mixed DMPC-d_{54}/h-cholesterol bilayer at $E = -0.2$ V. Abbreviation a.u. denotes absorbance units.

overtone bands (55,67). The band assignment and deconvolution are shown in Fig. 8 *b*.

For the sake of comparison with the νs(CH2) band, the νs(CD2) band frequency is plotted as a function of the electrode potential in Fig. 5 *a*. At the most negative potentials, where the mixed bilayer is detached from the metal surface, the $\nu_s(CD_2)$ band center is located at $\sim$2097 $\pm$ 1 cm^{-1}. At $E > -0.4$ V, where the bilayer is adsorbed on the Au (111) surface, the band center moves by approximately four wavenumbers to $\sim$2094.5 $\pm$ 0.5 cm^{-1}. Clearly, the changes of the band position with potential are much more pronounced than for the h-DMPC/h-cholesterol mixture. In a CCl_4 solution of d-DMPC/cholesterol, the position of the νs(CD2) band is 2098 cm^{-1}. In a dispersion of DMPC-d_{54}/h-cholesterol vesicles in H_2O, this band appears at 2090 cm^{-1}. The positions of the C-D stretch band indicate that the d-DMPC/h-cholesterol bilayer is in the liquid crystalline phase (68). However, the red shift of the band center in response to the change of the electrode potential from $E < -0.4$ V to $E > -0.4$ V, indicates that the acyl chains in the bilayer adsorbed at the metal surface contain fewer *gauche* conformations than in the desorbed bilayer.

The FWHM of the νs(CD2) band is plotted against the electrode potential in Fig. 5 *b*. The bandwidth changes from $\sim$12 cm^{-1} at the most negative potentials to $\sim$17 cm^{-1} at the most positive potentials. These numbers may be compared with 19 and 14 cm^{-1} corresponding to the FWHM of the νs(CD2) band in the solution of DMPC-d_{54}/h-cholesterol mixture in CCl_4 and in the suspension of vesicles formed by this mixture in H_2O. In the bilayer supported at the electrode surface, the acyl chains of deuterated DMPC contain more *gauche* conformations but are less mobile than in the suspension of vesicles at negative potentials where the bilayer is in the desorbed state. At more positive potentials, in the adsorbed state, the chains have fewer *gauche* conformations but are more mobile. One can also note an increase of the bandwidth (and hence the chain mobility) at the adsorption/desorption potentials ~ -0.5 V. Overall, the changes of the chain conformation and the chain mobility with potential are much more profound for perdeuterated than for nondeuterated chains.

Fig. 8 *a* shows that the intensity of the C-D stretches in the bilayer supported at the electrode surface is much weaker than the intensity of these bands in a spectrum of a bilayer consisting of randomly oriented molecules, calculated from the transmission spectra of DMPC-d_{54}/h-cholesterol mixture in CCl_4 or from a spectrum of vesicles dispersed in H_2O. The integrated intensities of these bands can be used to calculate angles between the directions of the transition dipole moments of the $\nu_{as}(CD_2)$ and $\nu_s(CD_2)$ band and the surface normal. Fig. 9, *a* and *b*, plot the angles θ_s and θ_{as} as a function of the electrode potential. Interestingly, the values of θ_s for the CD_2 stretch agree within 4° with the angles reported in Fig. 6 *a* for the symmetric CH_2 stretch. However, the values of θ_{as} for the CD_2 band are significantly higher than θ_{as} for

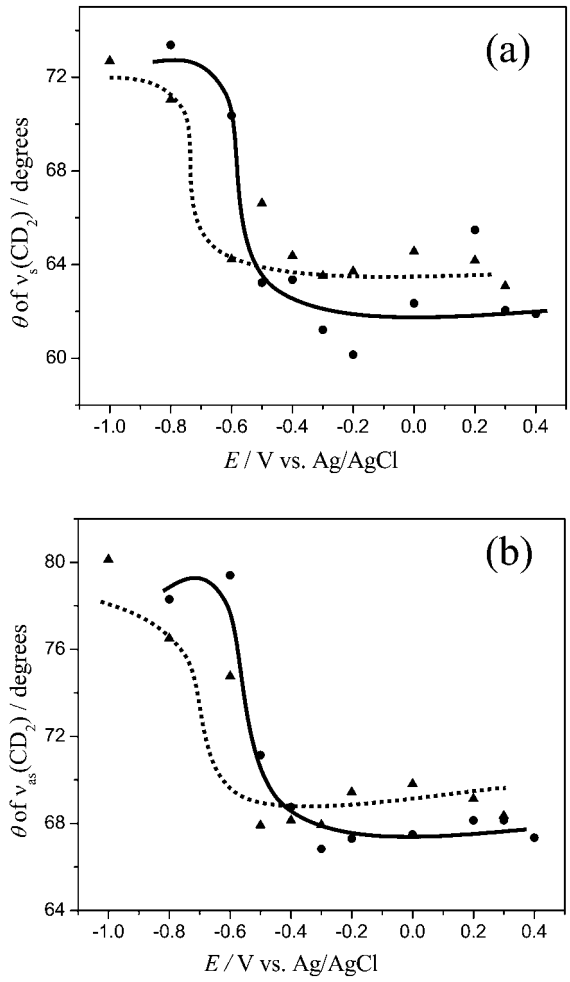

FIGURE 9 Dependence on the electrode potential of the angle (θ) between the direction of the transition dipole moment and the electric field of the photon (normal to the surface) for the mixed DMPC-d_{54}/h-cholesterol bilayer at an Au (111) electrode in 0.1 M NaF/H_2O solution; (*a*) ν_s (CD_2) and (*b*) $\nu_{as}(CD_2)$ band, (●) potential changed in the positive and (▲) potential changed in the negative direction.

CH_2 vibrations, shown earlier in Fig. 7 *a*. These differences reflect a different physical state of the bilayers formed by deuterated and nondeuterated DMPC.

Because the bilayer of deuterated DMPC is in the liquid-crystalline state, we cannot use Eq. 6 to calculate the chain tilt angle. However, the changes of θ_s and θ_{as} with potential suggest that the acyl chains of d-DMPC in the mixed bilayer are more tilted when the bilayer is directly adsorbed on the Au (111) electrode surface and less tilted when the bilayer is detached from the metal surface at more negative potentials. Clearly, the electric field-driven transformation of the DMPC-d_{54}/h-cholesterol bilayer is similar to the change observed for the h-DMPC/h-cholesterol bilayer. This is an important result. The processing of spectroscopic data involves background correction and band deconvolution procedures affected by systematic errors that are difficult to estimate. The fact that consistent physical information was obtained from

the analysis of IR bands located in different spectral regions indicates that these errors are small.

SUMMARY AND CONCLUSION

We have compared spreading of small unilamellar vesicles of pure DMPC and DMPC/cholesterol (7:3 molar ratio) at the Au (111) electrode surface by combined electrochemical and PM-IRRAS measurements. The charge density measurements provided the estimate of the potential drop across the membrane and energetics of the bilayer adsorption on gold. We have found that the bilayers are adsorbed (in direct contact with the metal) when the potential drop across the membrane is <0.4 V or the field acting at the membrane is $<\sim 6 \times 10^7$ V m^{-1}. When higher potentials (higher fields) are applied to the electrode, the bilayers are detached from the metal surface. Independent neutron reflectivity experiments (28) have shown that in the desorbed (detached) state the membrane remains in close proximity to the metal, separated by a ~1-nm-thick cushion of electrolyte.

The PM-IRRAS experiments provided information concerning the effect of the electric field on the orientation and conformation of DMPC molecules. At potentials where the bilayers are detached from the metal surface, the tilt of the acyl chains with respect to the surface normal is comparable with the tilt observed for bilayers in vesicles or in stacks of hydrated multibilayers. A dramatic increase of the tilt angle by 25–30° and a concomitant significant increase of the area per molecules is observed when the bilayer becomes adsorbed at the metal at fields $<6 \times 10^7$ V m^{-1}. The most pronounced changes in the tilt are observed between the adsorbed and desorbed (detached) states of the bilayer. Once the bilayer is adsorbed, a further change of the potential causes only a minor change of the tilt angle.

In the presence of cholesterol, the tilt angle and hence the area per DMPC molecule decrease. The addition of cholesterol leads also to an increase in the number of *gauche* conformations. These facts are consistent with the literature (1,8,64). However, we have discovered an interesting new phenomenon that cholesterol introduces much fewer *gauche* conformations in the adsorbed state than in the desorbed state of the bilayer. In the mixed DMPC/cholesterol bilayer, a significant conformational change of the acyl chains accompanies the potential-controlled phase transition from the desorbed to the adsorbed state of the bilayer. In contrast, in the bilayer of pure DMPC the conformational changes during the transition from the desorbed to the adsorbed state are negligible.

We have also shown that the mixed DMPC/cholesterol bilayer is characterized by a larger film pressure than the bilayer of pure DMPC. The bilayer with cholesterol is apparently energetically more stable and more compact when adsorbed at the metal surface. It constitutes a better matrix for the incorporation of peptides for further studies of the effect of the static electric field on the orientation and conformation of peptides and proteins.

This work was funded by a Natural Sciences and Engineering Research Council of Canada Discovery Grant. J.L. acknowledges the Canada Foundation of Innovation for a Canada Research Chair Award.

REFERENCES

1. Yeagle, P. L. 1985. Cholesterol and the cell membrane. *Biochim. Biophys. Acta.* 822:267–287.
2. Papahadjopoulos, D., S. Nir, and S. Ohki. 1971. Permeability of phospholipid membranes: effect of cholesterol and temperature. *Biochim. Biophys. Acta.* 266:561–583.
3. Corvera, E., O. G. Mouritsen, M. A. Singer, and M. J. Zuckermann. 1992. The permeability and the effect of acyl-chain length for phospholipid bilayers containing cholesterol: theory and experiment. *Biochim. Biophys. Acta.* 1107:261–270.
4. Kraske, W. V., and D. B. Mountcastle. 2001. Effects of cholesterol and temperature on the permeability of dimyristoylphosphatidylcholine bilayers near the chain melting phase transition. *Biochim. Biophys. Acta.* 1514:159–164.
5. Kuo, A.-L., and C. G. Wade. 1979. Lipid lateral diffusion by pulsed nuclear magnetic resonance. *Biochemistry.* 18:2300–2309.
6. Filippov, A., G. Orädd, and G. Lindblom. 2003. The effect of cholesterol on the lateral diffusion of phospholipids in oriented bilayers. *Biophys. J.* 84:3079–3086.
7. Semer, R., and E. Gelerinter. 1979. A spin label study of the effects of sterols on egg lecithin bilayers. *Chem. Phys. Lipids.* 23:201–211.
8. Umemura, J., D. G. Cameron, and H. H. Mantsch. 1980. A Fourier transform infrared spectroscopic study of the molecular interaction of cholesterol with 1,2-dipalmitoyl-*sn*-glycerol-3-phosphocholine. *Biochim. Biophys. Acta.* 602:32–44.
9. Silvius, J. R., D. D. Giudice, and M. Lafleur. 1996. Cholesterol at different bilayer concentration can promote or antagonize lateral segregation of phospholipids of differing acyl chain length. *Biochemistry.* 35:15198–15208.
10. Vist, R. M., and H. J. Davis. 1990. Phase equilibria of cholesterol/dipalmitoylphosphatidylcholine mixtures: ^{2}H nuclear magnetic resonance and differential scanning calorimetry. *Biochemistry.* 29:451–464.
11. Finegold, L. editor. 1990. Cholesterol in Membrane Models. CRC Press, Boca Raton, FL.
12. Borchman, D., R. J. Cenedella, and O. P. Lamba. 1996. Role of cholesterol in the structural order of lens membrane lipids. *Exp. Eye Res.* 62:191–197.
13. Estep, T. N., D. B. Mountcastle, R. L. Biltonen, and T. E. Thompson. 1978. Studies on the anomalous thermotropic behavior of aqueous dispersions of dipalmitoylphosphatidylcholine-cholesterol mixtures. *Biochemistry.* 17:1984–1988.
14. Mabrey, S., P. I. Mateo, and M. Sturtevant. 1978. High-sensitivity scanning calorimetric study of mixtures of cholesterol with dimyristoyl- and dipalmitoylphosphatidylcholines. *Biochemistry.* 17:2464–2468.
15. Ipsen, J. H., G. Karlström, O. G. Mouritsen, H. Wennerström, and M. J. Zuckermann. 1987. Phase equilibria in the phosphatidylcholine-cholesterol system. *Biochim. Biophys. Acta.* 905:162–172.
16. Lewis, R. N. A. H., N. Mak, and R. N. McElhaney. 1987. A differential scanning calorimetric study of the thermotropic phase behavior of model membranes composed of phosphatidylcholines containing linear saturated fatty acyl chains. *Biochemistry.* 26:6118–6126.
17. Mortensen, K., W. Pfeiffer, E. Sackmann, and W. Knoll. 1988. Structural properties of a phosphatidylcholine-cholesterol system as

studied by small-angle neutron scattering: ripple structure and phase diagram. *Biochim. Biophys. Acta.* 945:221–245.

18. McMullen, T. P. W., R. N. A. H. Lewis, and R. N. McElhaney. 1993. Differential scanning calorimetric study of the effect of cholesterol on the thermotropic phase behavior of a homologous series of linear saturated phosphatidylcholines. *Biochemistry.* 32:516–522.
19. Huang, T.-H., W. B. Lee, S. K. Das Gupta, A. Blume, and R. G. Griffin. 1993. A ^{13}C and ^{2}H nuclear magnetic resonance study of phosphatidylcholine/cholesterol interactions: characterization of liquid-gel phases. *Biochemistry.* 32:13277–13287.
20. McMullen, T. P. W., and R. N. McElhaney. 1995. New aspects of the interaction of cholesterol with dipalmitoylphosphatidylcholine bilayers as revealed by high-sensitivity differential scanning calorimetry. *Biochim. Biophys. Acta.* 1234:90–98.
21. Sáez-Cirión, A., A. Alonso, F. M. Goñi, T. P. W. McMullen, R. N. McElhaney, and E. A. Rivas. 2000. Equilibrium and kinetics studies of the solubilization of phospholipid-cholesterol bilayers by C12E8. The influence of the lipid phase structure. *Langmuir.* 16:1960–1968.
22. Loura, L. M. S., A. Fedorov, and M. Prieto. 2001. Exclusion of a cholesterol analog from the cholesterol-rich phase in model membranes. *Biochim. Biophys. Acta.* 1511:236–243.
23. McConnell, H. M., and M. Vrljic. 2003. Liquid-liquid immiscibility in membranes. *Annu. Rev. Biophys. Biomol. Struct.* 32:469–492.
24. Tsong, T. Y., and R. D. Astumian. 1988. Electroconformational coupling: how membrane-bound ATPase transduces energy from dynamic electric field. *Annu. Rev. Physiol.* 50:273–290.
25. Horswell, S. L., V. Zamlynny, H.-Q. Li, R. Merrill, and J. Lipkowski. 2002. Electrochemical and PM-IRRAS studies of potential controlled transformations of phospholipid layers on Au (111) electrodes. *Faraday Discuss.* 121:405–422.
26. Zawisza, I., A. Lachenwitzer, V. Zamlynny, S. L. Horswell, J. D. Goddard, and J. Lipkowski. 2003. Electrochemical and photon polarization modulation infrared refection absorption spectroscopy study of the electric field driven transformations of a phospholipid bilayer supported at a gold electrode surface. *Biophys. J.* 85:4055–4075.
27. Zawisza, I., X. Bin, and J. Lipkowski. 2004. Spectroelectrochemical studies of bilayers of phospholipids in gel and liquid state on Au(111) electrode surface. *Bioelectrochemistry.* 63:137–147.
28. Burgess, I., S. L. Horswell, G. Szymanski, J. Lipkowski, J. Majewski, and S. Satija. 2004. Electric field-driven transformations of a supported model biological membrane: an electrochemical and neutron reflectivity study. *Biophys. J.* 86:1763–1776.
29. Bin, X., I. Zawisza, J. D. Goddard, and J. Lipkowski. 2005. Electrochemical and PM-IRRAS studies of the effect of the static electric field on the structure of the DMPC bilayer supported at a Au (111) electrode surface. *Langmuir.* 21:330–347.
30. Barenholz, Y., D. Gibbes, and B. J. Litman. 1977. A simple method for the preparation of homogeneous phospholipids vesicles. *Biochemistry.* 16:2806–2810.
31. Dickertmann, D., J. W. Schultze, and F. D. Koppitz. 1976. A method to eliminate side effects in electrochemical measurements with single crystals. *Electrochim. Acta.* 21:967–971.
32. Richer, J., and J. Lipkowski. 1985. Measurement of physical adsorption of organic species at solid electrodes. *J. Electrochem. Soc.* 133:121–128.
33. Zawisza, I., X. Cai, V. Zamlynny, I. Burgess, J. Majewski, G. Szymanski, and J. Lipkowski. 2004. New methods to study thin organic films at electrode surfaces. *Pol. J. Chem.* 78:1165–1181.
34. Green, M. J., B. J. Barner, and R. M. Corn. 1991. Real time sampling electronics for double modulation experiments with Fourier transform infrared spectrometers. *Rev. Sci. Instrum.* 62:1426–1430.
35. Buffeteau, T., B. Desbat, D. Blaudez, and J. Turlet. 2000. Calibration procedure to derive IRRAS spectra from PM IRRAS spectra. *Appl. Spectrosc.* 54:1646–1650.
36. Zamlynny, V., I. Zawisza, and J. Lipkowski. 2003. PM FTIRRAS studies of potential-controlled transformations of a monolayer and a bilayer of 4-pentadecylpyridine, a model surfactant, adsorbed on a Au(111) electrode surface. *Langmuir.* 19:132–145.
37. Allara, D. L., and J. D. Swalen. 1982. An infrared reflection spectroscopy study of oriented cadmium arachidate monolayer films on evaporated silver. *J. Phys. Chem.* 86:2700–2704.
38. Li, N., V. Zamlynny, J. Lipkowski, F. Henglein, and B. Pettinger. 2002. In situ IR reflectance absorption spectroscopy studies of pyridine adsorption at the Au(110) electrode surface. *J. Electroanal. Chem.* 524–525:43–53.
39. Frey, S., and L. K. Tamm. 1991. Orientation of melithin in phospholipid bilayer: a polarized attenuation total reflection infrared study. *Biophys. J.* 60:922–930.
40. Flasch, C. R., A. Gericke, and R. Mendelsohn. 1997. Quantitative determination of molecular chain tilt angles in monolayer films at the air-water interface: infrared reflection absorption spectroscopy of bohenic acid methylester. *J. Phys. Chem. B.* 101:58–65.
41. Palik, E. 1998. Handbook of Optical Constants of Solid II, 2nd Ed. Academic Press, San Diego, CA.
42. Bertie, J., M. K. Ahmed, and H. H. Eysel. 1989. Infrared intensities of liquids. 5. Optical and dielectric constants, integrated intensities and dipole moment derivatives of H_2O and D_2O at 22°C. *J. Phys. Chem.* 93:2210–2218.
43. Léonard, A., C. Escrive, M. Laguerre, E. Pebay-Peyroula, W. Néri, T. Pott, J. Katsaras, and E. J. Dufourc. 2001. Location of cholesterol in DMPC membranes. A comparative study by neutron diffraction and molecular mechanics simulation. *Langmuir.* 17:2019–2030.
44. Bizzotto, D., V. Zamlynny, I. Burgess, C. A. Jeffrey, H. Q. Li, J. Rubinstein, Z. Galus, A. Nelson, B. Pettinger, A. R. Merill, and J. Lipkowski. 1999. Amphiphilic and ionic surfactants at electrode surfaces. *In* Interfacial Electrochemistry, Theory, Experiment and Applications. A. Wieckowski, editor. Marcel Dekker, New York, NY. 405–426.
45. Lipkowski, J., and L. Stolberg. 1992. *In* Adsorption of Molecules at Metal Electrodes. J. Lipkowski and P. N. Ross, editors. VCH Publishers, New York, NY. Chapt. 4. 171–238.
46. Li, M., B. Pettinger, and J. Lipkowski. 2005. Electrochemical and AFM studies of spreading DMPC vesicles at a Au(111) electrode surface. *Langmuir.* In press.
47. McMullen, T. P., R. N. Lewis, and R. N. McElhaney. 1994. Comparative differential scanning calorimetric and FTIR and 31P-NMR spectroscopic studies of the effects of cholesterol and androstenol on the thermotropic phase behavior and organization of phosphatidyl choline bilayers. *Biophys. J.* 66:741–752.
48. Becucci, L., M. R. Moncelli, R. Herrero, and R. Guidelli. 2000. Dipole potentials of monolayers of phosphatidylcholine, phosphatidylserine and phosphatic acid on mercury. *Langmuir.* 16:7694–7700.
49. Sandblom, J., A. Galvanovskis, and B. Jilderos. 2001. Voltage-dependent formation of gramicidin channels in lipid bilayers. *Biophys. J.* 81:827–837.
50. Lipkowski, J., C. Nguyen, V. Huong, C. Hinnen, R. Parsons, and J. J. Chevalet. 1983. Adsorption of diethylether on single crystal gold electrodes. Calculation of adsorption parameters. *Electroanal. Chem.* 143:375–396.
51. Brockman, H. 1994. Dipole potential of lipid membranes. *Chem. Phys. Lipids.* 73:57–79.
52. Clarke, R. J. 1997. Effect of lipid structure on the dipole potential of phosphatidylcholine bilayers. *Biochim. Biophys. Acta.* 1327:269–278.
53. Guidelli, R., G. Aloisi, L. Becucci, A. Dolfi, M. R. Moncelli, and F. T. Bouninsegni. 2001. Bioelectrochemistry at metal-water interfaces. *J. Electroanal. Chem.* 504:1–28.
54. MacPhail, R. A., H. L. Strauss, R. G. Snyder, and C. A. Elliger. 1984. C-H stretching modes and the structure of n-alkyl chains. 2. Long, all-trans chains. *J. Phys. Chem.* 88:334–341.

55. Lewis, R. N. A. H., and R. N. McElhaney. 1996. *In* Infrared Spectroscopy of Biomolecules. H. H. Mantsch and D. Chapman, editors. Wiley-Liss, New York, NY. 159–202.

56. Snyder, R. G., S. L. Hsu, and S. Krimm. 1977. Vibrational spectra in the C-H stretching region and the structure of the polymethylene chain. *Spectrochim. Acta.* 34:395–406.

57. Cameron, D. G., H. L. Casal, and H. H. Mantsch. 1980. Characterization of the pretransition in 1,2-dipalmitoyl-sn-glycero-3-phosphocholine by Fourier transform infrared spectroscopy. *Biochemistry.* 19:3665–3672.

58. Snyder, R. G., H. L. Strauss, and C. A. Elliger. 1982. C-H stretching modes and the structure of *n*-alkyl chains. 1. Long, disordered chains. *J. Phys. Chem.* 86:5145–5150.

59. Brandenburg, K., and R. G. Snyder. 1986. Orientation measurement on ordered multibilayers of phospholipids and sphingolipids from synthetic and natural origin by ATR Fourier transform infrared spectroscopy. *Z. Naturforsch.* 41c:453–467.

60. Heimburg, T. 2000. A model for the lipid pretransition: coupling of ripple formation with the chain-melting transition. *Biophys. J.* 78: 1154–1165.

61. Allara, D. L., and R. G. Nuzzo. 1985. Spontaneously organized molecular assemblies. 2. Quantitative infrared spectroscopic determination of equilibrium structures of solution-adsorbed n-alkanoic acids on an oxidized aluminum surface. *Langmuir.* 1:52–66.

62. Fringeli, U. P. 1977. The structure of lipids and proteins studied by attenuated total reflection (ATR) infrared spectroscopy. *Z. Naturforsch.* 32b:20–45.

63. Umemura, J., T. Kamata, T. Kawai, and T. Takenaka. 1990. Quantitative evaluation of molecular orientation in thin Langmuir-Blodgett films by FT-IR transmission and reflection-absorption spectroscopy. *J. Phys. Chem.* 94:62–67.

64. McIntosh, T. J. 1978. The effect of cholesterol on the structure of phosphatidylcholine bilayers. *Biochim. Biophys. Acta.* 513:43–58.

65. Knoll, W., K. Ibel, and E. Sackmann. 1981. Small-angle neutron scattering study of lipid phase diagrams by the contrast variation method. *Biochemistry.* 20:6379–6383.

66. Janiak, M. J., D. M. Small, and G. G. Shipley. 1979. Temperature and compositional dependence of the structure of hydrated dimyristoyl lecitin. *J. Biol. Chem.* 254:6068–6078.

67. Sunder, S., D. Cameron, H. H. Mantsch, and H. J. Bernstein. 1978. Infrared and laser Raman studies of deuterated model membranes: phase transition in 1,2-perdeuterodipalmitoyl-*sn*-glycero-3-phosphocholine. *Can. J. Chem.* 56:2121–2126.

68. Khalil, M. B., M. Kates, and D. Carrier. 2000. FTIR study of the monosialoganglioside GM_1 in perdeuterated dimyristoylglycerophosphocholine (DMPC) multilamellar bilayers: spectroscopic evidence of a significant interaction between Ca^{2+} ions and the sialic acid moiety of GM_1. *Biochemistry.* 39:2980–2988.